Journal of Nuclear Materials 401 (2010) 46–54

Contents lists available at ScienceDirect

Journal of Nuclear Materials

journal homepage: www.elsevier.com/locate/jnucmat

Optimisation of the hot conditioning of carbon steel surfaces of primary heat transport system of Pressurized Heavy Water Reactors using electrochemical impedance spectroscopy

M. Kiran Kumar [a,*], Krishna Gaonkar [a], Swati Ghosh [a], Vivekanand Kain [a], Martin Bojinov [b], Timo Saario [c]

[a] Materials Science Division, Bhabha Atomic Research Centre, Mumbai 400 085, India
[b] Department of Physical Chemistry, University of Chemical Technology and Metallurgy, Kl. Ohridski Blvd. 8, 1756 Sofia, Bulgaria
[c] VTT Materials and Building, VTT Technical Research Centre of Finland, P.O. Box 1000, Kemistintie 3, FIN-02044 VTT, Espoo, Finland

ARTICLE INFO

Article history:
Received 10 November 2009
Accepted 23 March 2010

ABSTRACT

Hot conditioning operation of the primary heat transport system is an important step prior to the commissioning of Pressurized Heavy Water Reactors. One of the major objectives of the operation is to develop a stable and protective magnetite layer on the inner surfaces of carbon steel piping. The correlation between stable magnetite film growth on carbon steel surfaces and the period of exposure to hot conditioning environment is generally established by a combination of weight change measurements and microscopic/morphological observations of the specimens periodically removed during the operation. In the present study, electrochemical impedance spectroscopy (EIS) at room temperature is demonstrated as an alternate, quantitative technique to arrive at an optimal duration of the exposure period. Specimens of carbon steel were exposed for 24, 35 and 48 h during hot conditioning of primary heat transport system of two Indian PHWRs. The composition and morphology of oxide films grown during exposure was characterized by X-ray diffraction and optical microscopy. Further, ex situ electrochemical impedance spectra of magnetite films formed after each exposure were measured, in 1 ppm Li^+ electrolyte at room temperature as a function of potential in a range of −0.8 to +0.3 V_{SCE}. The defect density of the magnetite films formed after each exposure was estimated by Mott–Schottky analysis of capacitances extracted from the impedance spectra. Further the ionic resistance of the oxide was also extracted from the impedance spectra. Defect density was observed to decrease with increase in exposure time and to saturate after 35 h, indicating stabilisation of the barrier layer part of the magnetite film. The values of the ionic transport resistance start to increase after 35–40 h of exposure. The quantitative ability of EIS technique to assess the film quality demonstrates that it can be used as a supplementary tool to the thickness and morphological characterizations of samples during hot conditioning.

1. Introduction

The main material of construction for the recirculation pipelines in the primary heat transport (PHT) system of Pressurized Heavy Water Reactors (PHWRs) is carbon steel (CS). These pipes in service are exposed to high-temperature (inlet and outlet temperatures being 249 °C and 292 °C, respectively) and high pressure heavy water for long durations [1–5]. The water chemistry is alkaline (pH ranging from 10 to 10.3) in nature and dissolved oxygen levels are maintained at very low levels (<5 ppb) [1–5]. The corrosion behaviour of pure iron and carbon steel in high-temperature water electrolytes has been studied quite extensively in recent years [5–25]. The corrosion of carbon steel under the above conditions results in the formation of an adherent, compact and uniform oxide layer with a composition Fe_3O_4 (magnetite) [6–9]. There are evidences of Fe_3O_4 getting partly oxidised to loose or non-protective oxides such as Fe_2O_3/FeOOH, at higher potentials when the dissolved oxygen level in the water is increased [10,24]. By oxidising pure iron in atmospheric air at a temperature of 200–300 °C, well-defined duplex films comprised of a magnetite (Fe_3O_4) inner sublayer and a hematite (Fe_2O_3) outer layer are formed [26–31]. In an oxygen deficient atmosphere, like N_2, the formation of a pure magnetite scale was promoted [26–28]. Magnetite and hematite have completely different structures. Magnetite exhibits a cubic close packed arrangement of oxygen ions with octahedral and tetrahedral interstices occupied by Fe^{3+} and some of the octahedral sites occupied by Fe^{2+} ions as well. On the other hand hematite has a hexagonal close packed array of oxygen with the octahedral sites being occupied predominantly by Fe^{3+} ions.

In order to ensure the presence of a protective and adherent layer of magnetite on the carbon steel surfaces before they are

* Corresponding author.
E-mail address: mkiran@barc.gov.in (M. Kiran Kumar).

0022-3115/$ - see front matter © 2010 Elsevier B.V. All rights reserved.
doi:10.1016/j.jnucmat.2010.03.017

introduced into actual service, a hot conditioning operation is performed prior to the commissioning of a PHWR. The hot conditioning operation involves exposing the PHT system to light water under controlled conditions of temperature, pressure, flow rate and water chemistry. The objectives of hot conditioning are: (a) to check the system integrity and leakage of coolant at high pressure conditions and (b) to develop an adherent and protective magnetite layer on the inner surfaces of carbon steel pipings/components and consequently minimizing further corrosion, crud release and base metal loss during reactor operation [1–5]. This in turn minimizes the activity build-up and activity transport during operation.

Achieving the second objective necessitates a method of evaluation of the carbon steel surfaces at different exposure times to monitor the nature of the oxide film formed on them. This helps in optimising an exposure period that ensures the presence of a protective, adherent magnetite film. For this purpose, CS coupons are suspended in autoclaves specially installed in line with the recirculating PHT system, so that they are exposed to similar water chemistry parameters as the pipes themselves. These CS coupons are subsequently evaluated by a combination of microscopic observations, to assess the morphology and uniformity in coverage of the film, and weight change leading to the estimation of oxide thickness and base metal corrosion [1–5].

Another quantitative way of evaluation of the corrosion coupons after different periods of exposure to hot conditioning water may lie in the context of determining the electronic and ionic transport properties of the oxide layer formed on it. Both magnetite and hematite behave like n-type semiconductors due to point defects in the oxide structure [32], like Fe^{2+} ions in the Fe^{3+} matrix and O^{2-} vacancies. It is well known that these defects play an important role in the corrosion of metals, influencing the transport through the oxide layer [5,20,33–34]. The conductivity of hematite is very low compared to magnetite because of the very low defect density, the main donor states being Fe^{2+} and oxygen vacancies [26–28]. It has been argued on the basis of electrochemical and photo electrochemical measurements [20,21] that these properties are controlled by a thin (a few nm) semiconductor layer (barrier layer) regardless of the fact that the overall film thickness can reach several micrometers. The semiconductor film in contact with the electrolyte develops a space charge layer. Mott–Schottky analysis of the potential dependence of capacitances extracted from Electrochemical Impedance Spectroscopy (EIS) measurements is a suitable method to estimate the defect densities in the film [32].

In the present work, CS coupons exposed for different durations during hot conditioning of an Indian PHWR were studied. The oxide formed on carbon steel during these exposures was evaluated mainly by EIS at room temperature and at different applied potentials followed by Mott–Schottky analysis to estimate the defect densities in the oxide. In addition, X-ray diffraction and optical microscopic studies were also carried out to assess the morphologies and the phases present. Based on the estimated defect density values and their evolution with exposure time, conclusions are drawn on the protective nature of the oxide film and the optimum duration of exposure to the hot conditioning environment that is required to develop such a film. These estimates are further compared with results obtained from conventional ways of evaluation by weight change technique and earlier results from in situ measurement of EIS on CS in simulated Hot Conditioning environment [5].

2. Experimental

2.1. Material

In the present work, ASTM-A-333 Grade-6 carbon steel (see Table 1 for chemical composition) with oxide layer on the surface was studied. The oxide layer on CS was grown by exposure of coupons (dimensions 30 × 15 × 1 mm with a hole of 3 mm diameter at both ends) to recirculating water in the PHT system during hot conditioning of two Indian PHWRs. These coupons were polished up to 600 grit emery paper before loading in the stringers (specimen holders).

2.2. Hot Conditioning

Hot conditioning of the PHT system was performed with light demineralized (DM) water. The chemistry of the water was strictly controlled throughout the operation and the parameters are mentioned in Table 2. Two autoclaves (50 mm nominal inner diameter) were installed in line with the main circulation piping of the PHT system. Coupons of CS held in specially designed specimen holders (stringers) were introduced in the autoclave at 150 °C and beginning of hot conditioning was considered when the system attained 185 °C (as the oxidation of carbon steel is significant at and above these temperatures). Coupons were periodically taken out after different exposure times (after attainment of 185 °C) varying from 24 to 48 h and were characterized by optical microscopy and electrochemical impedance spectroscopy. The maximum temperature of about 230 °C was achieved within the first 3 h of exposure and the pressure in the main circulation system was ~7 MPa. A flow of ~40 $dm^3\ min^{-1}$, resulting in a flow velocity of 1–2 $m\ s^{-1}$ was maintained through the autoclave. Fig. 1 shows the Pourbaix-diagram (phase stability diagram) for Fe-H_2O-system at 230 °C. The red square marks the conditions during the hot conditioning (pH (230 °C) = 7.3 and $-0.7\ V < E_{SHE} < -0.6\ V$), indicating predominance of magnetite, Fe_3O_4.

2.3. Characterization of structure and morphology

The coupons removed after each interval were cleaned ultrasonically and observed under optical microscope to assess the uniformity in coverage of the oxide layer. X-ray diffraction patterns for plain polished (blank) and magnetite coated carbon steel coupons were obtained by using X-ray wave length of Cu $K\alpha_1$ 1.5406 Å.

2.4. Electrochemical impedance spectroscopy and Mott–Schottky analysis

The impedance spectra were measured with Solartron 1287/1260 at room temperature in electrolyte (DM water with 1 ppm Li^+) using ac amplitude of 5 mV in the frequency range between

Table 1
Typical chemical composition of ASTM-A-333 Grade-6 carbon steel used for exposure to hot conditioning environment.

Material	Grade	Nominal composition (wt.%)
Carbon steel	ASTM-A-333 Grade-6	C-0.3, Mn-0.3, P-0.05, S-0.06, Si-0.1, and Fe-balance

Table 2
Water chemistry parameters during hot conditioning.

pH	10.2 at 25 °C, corresponding to 7.3 at 230 °C (by adding 1 ppm Li^+ as LiOH)
Conductivity at 25 °C, $\mu S\ cm^{-1}$	On the average about 60
Dissolved oxygen, $\mu g\ dm^{-3}$	<5
Chloride, mg dm^{-3}	<0.2
Crud, mg dm^{-3}	140 to begin with and <0.1 at the end
Hydrazine, mg dm^{-3}	5 to begin with and <0.2 at the end

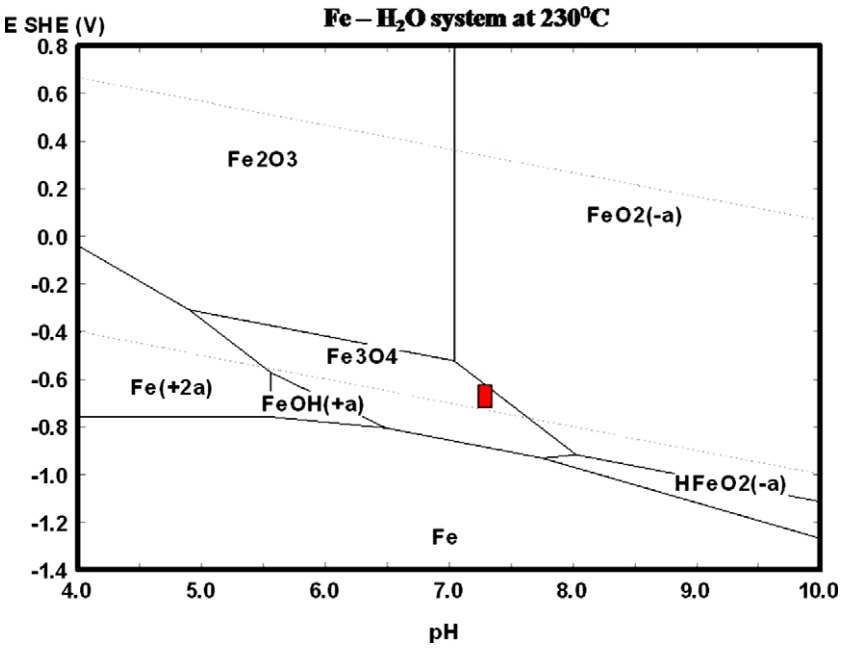

Fig. 1. Pourbaix-diagram of Fe-H_2O system at 230 °C. The red square shows the conditions, where the hot conditioning is occurring, i.e. pH (230 °C) = 7.3 (for 1 ppm Li^+) and $-0.7\ V < E_{SHE} < -0.6\ V$ (for totally deoxygenated conditions). (For interpretation of the references to colour in this figure legend, the reader is referred to the web version of this article.)

10^6 and 10^{-2} Hz. Oxygen was removed by continuous bubbling with Argon gas and measurement was started after bubbling for a minimum of 1 h. For Mott–Schottky analysis, the spectra were taken as a function of potential (with respect to saturated calomel electrode, SCE), in a potential range of $-0.8\ V_{SCE}$ to $+0.3\ V_{SCE}$, in 0.1 V steps. The potential range was chosen such that it remains within the stability area of water at the pH of 10.4 at 25 °C, see Fig. 1 for the Pourbaix-diagram of Fe-H_2O system. A pre-treatment/waiting time of 15 min was applied at each potential before starting the measurement. The resultant spectra were modelled using equivalent circuit (circuits described in Section 3.2) approach to estimate the capacitance (C) of the semiconducting oxide layer. The defect density was calculated from the slope of the linear part of the plot between $1/C^2$ and potential. Further details of Mott–Schottky analysis are explained in Section 3.2.

3. Results and discussion

3.1. Composition and morphology of the oxide layer

The X-ray diffraction (XRD) studies of the oxides grown on CS coupons after exposure to hot conditioning environment for different periods were carried out to assess the phases present on the CS surface. Fig. 2 shows X-ray diffractograms (using Cu Kα incident radiation) of carbon steel specimens before (Fig. 2a) and after exposure to hot conditioning for 24, 35, and 48 h (Fig. 2b–d). Peaks observed at 2θ of 44.66° and 64.97° correspond to α-Fe. These two peaks were observed in the XRD of blank CS specimen as well as in the specimens after each exposure. The XRD peaks at 2θ: 30.1° (d – 2.967 Å, hkl 220), 35.4° (d – 2.532 Å, hkl 311), 43.05° (d – 2.099 Å, hkl 400), 56.9° (d – 1.616 Å, hkl 511) and 62.5° (d – 1.484 Å, hkl 440) observed in oxide film on coupons removed after different periods of exposure correspond to the magnetite phase. It is to be noted that except magnetite and base metal peaks none of the specimens revealed peaks for any other iron oxide like hematite, goethite etc. This is an evidence for the presence of only magnetite phase on the carbon steel material. The presence of α-Fe peaks also on oxidised specimens can be attributed to the rather thin oxide film. The gradual enhancement in the intensity of magnetite peaks with increase in exposure period (see Fig. 2b–d) is indicative of the progressive build-up of magnetite layer on the CS surface. Therefore, it can be inferred from XRD studies that the hot conditioning process carried out under controlled water chemistry condition yielded the desired protective magnetite film.

The coverage of magnetite layer on the CS surface was additionally assessed by optical microscopy. Fig. 3a shows the surface finish of a typical plain polished CS coupon used during the hot conditioning. Fig. 3b (24 h) and c (35 h) show different stages of magnetite film build-up on CS surface during hot conditioning. After 24 h (Fig. 3b) of exposure the carbon steel surface was partially covered with a thin magnetite layer. The sub-surface corrosion was minimal. The carbon steel surface was fully covered with a thin, uniform and black magnetite film after 35 h (Fig. 3c) of exposure. For longer exposure periods, magnetite film thickness increased rather slowly and the carbon steel surface remained completely covered with uniform, thin, black, adherent and shining magnetite layer. In a few cases anomalous oxide growth behaviour was found. Fig. 3d shows a sample from Reactor-1 south after 23.5 h exposure. The oxide clearly is very uneven which then is also reflected as an anomalous result from impedance spectra (Fig. 8b). Impedance spectra from these cases were discarded from final analysis.

3.2. Electrochemical impedance spectroscopy (EIS)

The electrochemical impedance spectroscopic measurements were carried out on CS specimens exposed to the hot conditioning environment of the reactor. Following are the observations and explanations on the EIS results along with correlation with existing literature.

The raw data for the 24 h exposure coupon are shown in Fig. 4 as a Bode plot. All spectra exhibited a very high frequency peak (>100 kHz) in phase angle and another maximum at lower frequencies. It is to be noted that the high frequency peak did not show any change as a function of applied potential. Because of this it was suspected that it may be caused by the reference electrode. To check this, the measurement was repeated in two-electrode

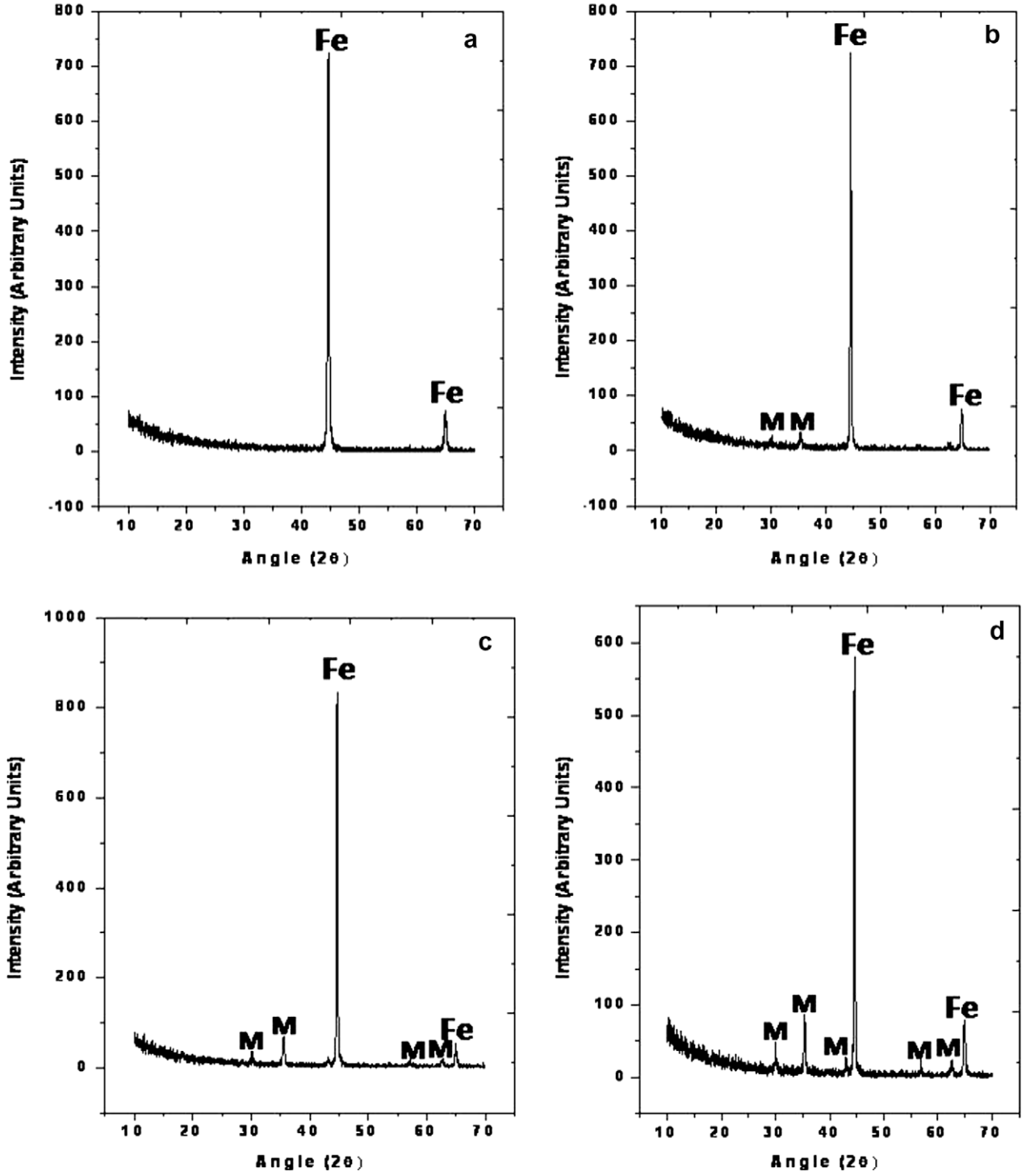

Fig. 2. X-ray diffraction patterns of: (a) blank carbon steel coupon before exposure and (b)–(d) after exposure to hot conditioning environment for 24, 35, and 48 h duration, respectively.

mode, in which the reference electrode was removed from the solution and the counter electrode was used both as a counter and a reference electrode. This resulted in almost total elimination of this high frequency peak, confirming that it was caused by the SCE. Hence for modelling the experimental spectra using equivalent circuit approach, only the lower frequency parts of the spectra (below 1 kHz) were considered. As a representative example, the lower frequency parts of the spectra obtained as a function of potential on the CS specimen exposed for 24 h are collected in Fig. 5. The fitting was carried out in general with an equivalent circuit shown in Fig. 6. In this circuit, DX is Young's impedance [35], which has been recently introduced in the Zview-software and is, by and large, used for modelling/fitting the impedance spectra of films the conductivity of which varies exponentially with depth. The second R-CPE-circuit was added with an aim to account for an interfacial process at the film/solution boundary. This process is hypothesised to be the oxidation of Fe^{2+}–Fe^{3+} within the magnetite film during the measurement of the impedance spectra.

The presented circuit is mathematically equivalent to a transfer function of the type [20]

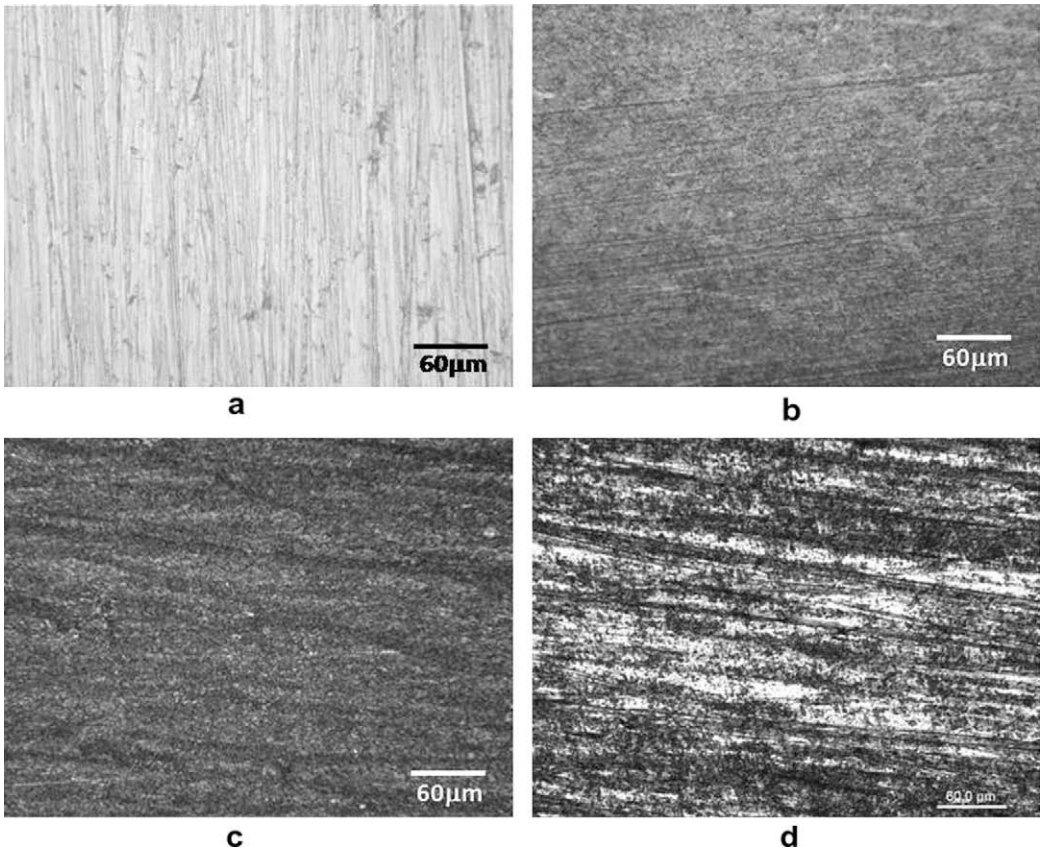

Fig. 3. Surface morphology by optical microscopy of: (a) blank CS coupon before exposure, (b) and (c) after exposure to hot conditioning environment for 24 and 35 h duration respectively, and (d) an example of non-representative very uneven oxide morphology (23.5 h Reactor-1 south).

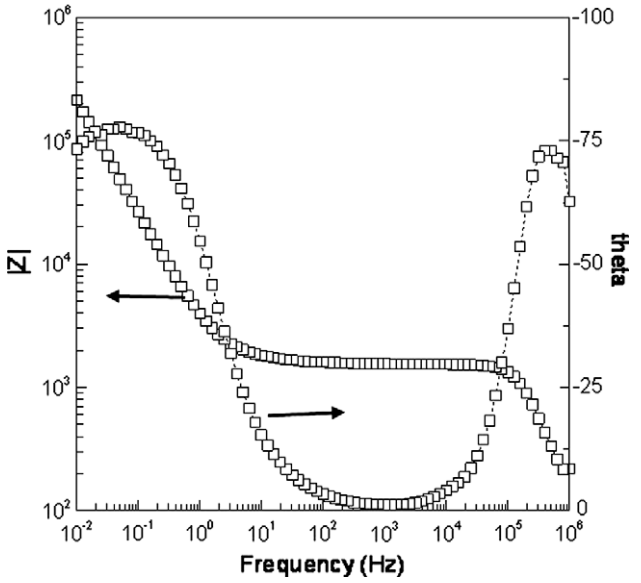

Fig. 4. Experimental electrochemical impedance spectrum (Bode plot) for magnetite grown on CS surface exposed to hot conditioning environment for 24 h duration. The spectrum shows both the high frequency (later attributed to the contribution from the reference electrode) and low frequency peaks.

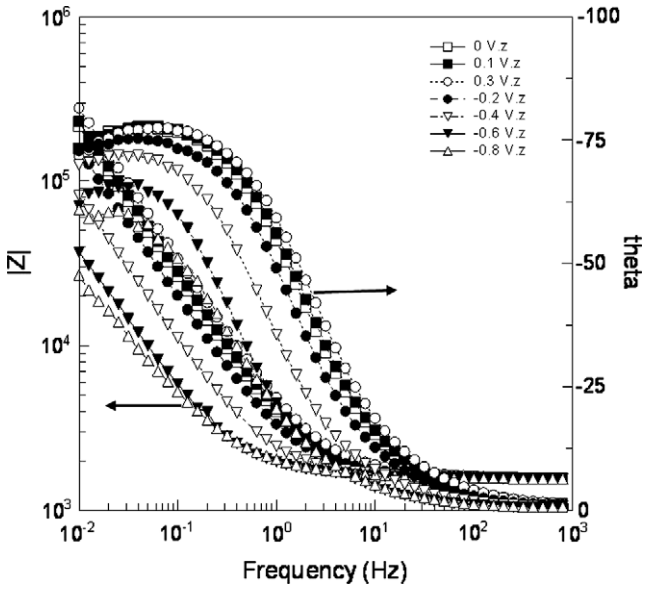

Fig. 5. Experimental EIS spectra (Bode plots) as a function of potential for CS surface exposed to hot conditioning environment for 24 h. The spectra were obtained in a solution of DM water with 1 ppm Li as LiOH (pH = 10.4) at room temperature in a potential range of −0.8 V_{SCE}–0.3 V_{SCE} with steps of 0.1 V.

$$Z = R_{el} + Z_{F/E} + Z_f$$
$$Z_{F/E} = \frac{1}{R_t^{-1} + (j\omega)^n C_{F/E}}, \quad Z_f = (Z_e^{-1} + R_{ion}^{-1})^{-1}, \tag{1}$$
$$Z_e = \frac{p}{j\omega C} \ln \frac{\left[1 + j\omega\rho_d \varepsilon\varepsilon_0 \exp\left(\frac{1}{p}\right)\right]}{1 + j\omega\rho_d\varepsilon\varepsilon_0}$$

where Z_e, the impedance describing the electronic properties of the inner layer, has the form of an Young impedance, ρ_d being the interfacial defect induced resistivity, C the depletion layer capacitance and p the relative depth of penetration of the conductivity profile [20]. On the other hand, R_{ion} is the resistance due to ionic transport

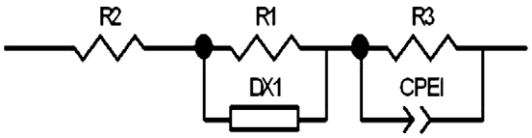

Fig. 6. The equivalent circuit used for modelling/fitting the experimental impedance spectra.

through the layer and $C_{F/E}$ and R_t can be interpreted as the interfacial capacitance and charge transfer resistance.

A comparison between an experimental (points) and a calculated spectrum (solid line) is shown in Fig. 7 as an example. The good fit with the experimental data does give confidence on the accuracy of the modelling procedure and the equivalent circuit used. It is worth mentioning that due to the overlap of the two time constants in the spectra, some of the parameters extracted from the fitting were computed with a large error and will not be commented further. In the subsequent discussion, we will focus on the capacitance of the depletion layer C and the resistance R_{ion} due to ionic transport through the layer.

Using the values of the depletion layer capacitance C as depending on the applied potential, Mott–Schottky plots were generated by plotting C^{-2} vs. E as shown in Fig. 8.

According to the Mott–Schottky equation,

$$C^{-2} = \left(\frac{2}{\varepsilon\varepsilon_0 e N_D}\right)\left|(E - E_{fb}) - \frac{kT}{e}\right| \tag{2}$$

The slope of such plot can be used to calculate the donor density N_D in the film. Here E_{fb} is the flat band potential, ε is the dielectric constant of the oxide, ε_0 is the permittivity in vacuum, e the unit charge and k the Boltzmann constant. In an iron oxide, interstitial Fe^{2+} or oxygen vacancies typically act as electron donors. Thus, the slope of the linear part of a Mott–Schottky plot can be used to obtain an approximation for the defect density in the oxide film. At very high positive potentials band bending in the semiconducting part of the oxide becomes so large that additional conduction mechanisms become possible which is seen as a deflection from the linear behaviour (Fig. 8).

From the intercepts of the straight lines in Fig. 8, the flat band potential can be estimated to be between $-0.4\ V_{SCE} < E_b < -0.5\ V_{SCE}$. The flat band potential measured by Wielant et al. [32] for magnetite oxide grown in N_2 gas environment at 250 °C with final thickness of about 0.1 μm was $E_b \approx -0.39\ V_{SCE}$. The small difference between Wielant et al. result and that found in the present study may reflect the difference in the pH of the electrolyte used (Wielant et al. used borate buffer solution with pH = 8.2 while the 1 ppm Li^+ solution used in this study had a pH = 10.4).

The slopes of the linear part of Mott–Schottky curves, see Fig. 9, were then used to estimate the defect densities for the oxides with various exposure times. The results in terms of defect densities in the oxide film as a function of exposure time to hot conditioning of both reactors are presented in Fig. 9 together with the results from the study of Wielant et al. [32]. The values indicate that the defect density in the magnetite film exposed to the Hot Conditioning environment stabilises after about 35 h exposure to a level close to $3 \times 10^{21}\ cm^{-3}$. This level is comparable to that estimated by Wielant et al. [32], notwithstanding the fact that their study involves electrochemical impedance spectroscopy on thermally grown (at 250 °C in an oven) magnetite on steel under an oxygen deficient N_2 atmosphere.

The dependences of the resistance of ionic transport, R_{ion}, on potential for CS specimens subject to hot conditioning in both reactors are shown in Fig. 10. It is worthwhile to mention that these plots are in fair agreement with the potential dependence of thermally formed oxides on iron as reported by Wielant et al. [32]. Following these authors, we could assume that a very thin layer of a higher-valency iron oxide (e.g. maghemite) was formed on top of the magnetite scale, and the ionic transport through it is limiting the overall resistance of the oxide. If the principal ionic current carriers in this layer are the mobile divalent iron interstitials in octahedral positions, formed during oxidation of Fe at the CS/oxide interface and further oxidised to trivalent iron

$$Fe_m Fe_i^{\cdot\cdot} + 2e_m^-$$
$$Fe_i^{\cdot\cdot} Fe_{aq}^{3+} + e_{oxide}^-$$

then according to the mixed-conduction model for oxide films, the reciprocal value of the ionic transport resistance will be given by the equation

$$R_{ion}^{-1} = \frac{4F^2 D_i}{RTa}(1-\alpha)\frac{k_{1i}^0}{k_{3i}^0} e^{-b_{3i}\alpha E} e^{-\frac{\bar{L}}{a}} + \frac{4F^2 D_i}{RTa}(1-\alpha)k_{1i}^0 \tag{3}$$

where $D_i = D_i e^{\frac{2F\alpha\bar{E}}{RT}}$ is the apparent (field dependent) diffusion coefficient of divalent iron interstitials, L is the higher-valency oxide

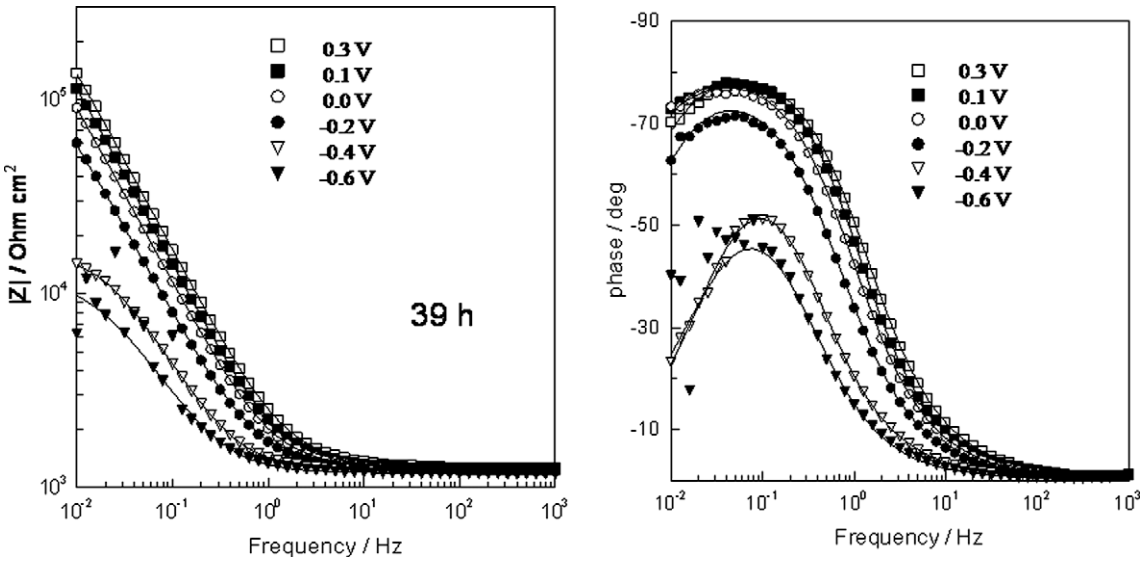

Fig. 7. Results on modelling the impedance spectrum for CS surface after 24 h exposure (shown as a representative picture) using the equivalent circuit described in Fig. 6.

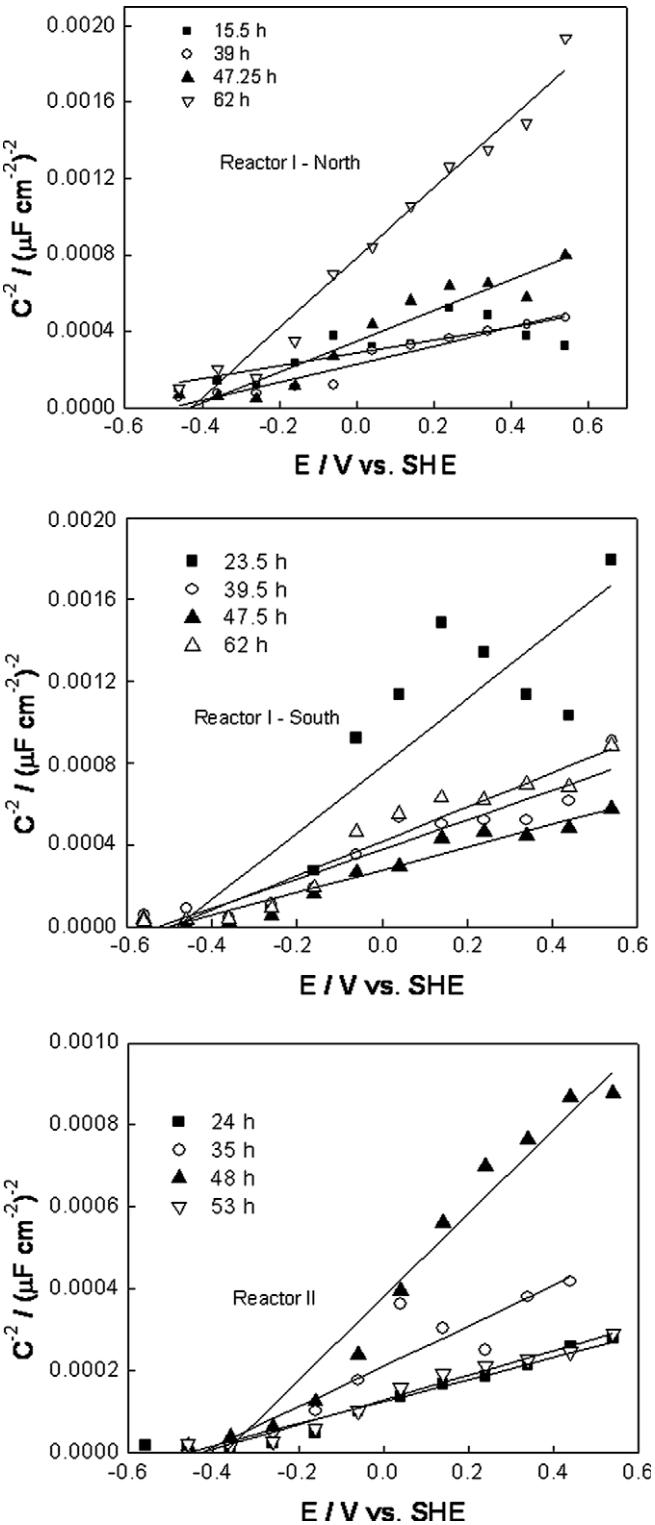

Fig. 8. Mott–Schottky plots, C^{-2} vs. E, for CS specimens exposed to hot conditioning environment for 15–62 h duration in different reactors. The capacitance (C) was derived through fitting of low frequency processes of the EIS by equivalent circuit approach.

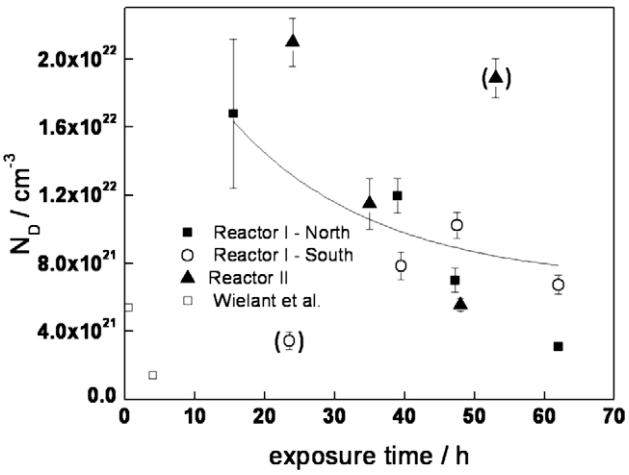

Fig. 9. Defect density values (N_D), in the magnetite film estimated through Mott–Schottky analysis of EIS data on CS coupons exposed to hot conditioning environment as a function of time. The values are presented for exposures in two PHWRs and data points from the study of Wielant et al. [32] for pure magnetite. Data based on samples with clearly uneven oxide morphology are shown in parentheses and are considered as non-representative.

thickness, α is the part of the applied potential consumed at the oxide/solution interface, and b_{3i} is the exponential coefficient of the oxidative dissolution reaction (step 3i) and a is the half-jump distance for a hopping ionic defect. It has been demonstrated by some of us [36] that Eq. (4) can account for the increase of the ionic transport resistance from the flatband potential to ca. 0 V and its subsequent stabilisation at higher potentials.

The dependence of the ionic transport resistance at a potential of 0.14 V (i.e. in the stabilisation region) on exposure time of CS specimens in the two reactors is shown in Fig. 11. Notwithstanding the scatter in the resistance values, a transition at ca. 35–40 h of exposure is observed also in the R_{ion} – t dependence in reasonable agreement with the donor density data (Fig. 9). For shorter exposures, the values of R_{ion} are relatively constant, whereas for exposures above 35–40 h, an increase in the values of that parameter is detected. Bearing in mind that the limiting value of R_{ion} at potentials higher than 0 V could be represented by

$$R_{ion} = \frac{RTa}{4F^2 D_i (1-\alpha) k_{1i}^0} a \qquad (4)$$

such an increase can be explained either by a decrease of the rate constant of formation or the diffusion coefficient of divalent iron interstitials. Either way, the increase of the ionic transport resistance can be interpreted by the formation of a more compact and less defective oxide on the CS specimens exposed to hot conditioning for more than 40 h.

Summarising, the results of the present study suggest that an exposure of CS tubings to hot conditioning environment for a period of at least 35 h produces a stable magnetite layer on the tube internal surfaces. The stable oxide layer thus formed is also protective in nature as indicated by the level of defect densities present in the film, which are close to the values estimated for pure magnetite [32], and the ionic transport resistance through the oxide, which is observed to increase. The morphological studies through optical microscopy (see Fig. 3 and Section 3.1) also support such an observation. The magnetite film grown on CS surface does show lack of complete coverage up to 24 h of exposure, while the specimen exposed for 35 h shows a complete and uniformly covered magnetite layer over the CS surface. Such observation is well in agreement with and supplements well to our earlier studies [4–5] in terms of weight gain/thickness estimation. The results of these earlier studies [4–5] suggested that magnetite growth follows a parabolic rate law, and the film growth stabilises after an exposure of about 30 h to the hot conditioning environment, base metal corrosion beyond this exposure being minimal [4–5]. In a

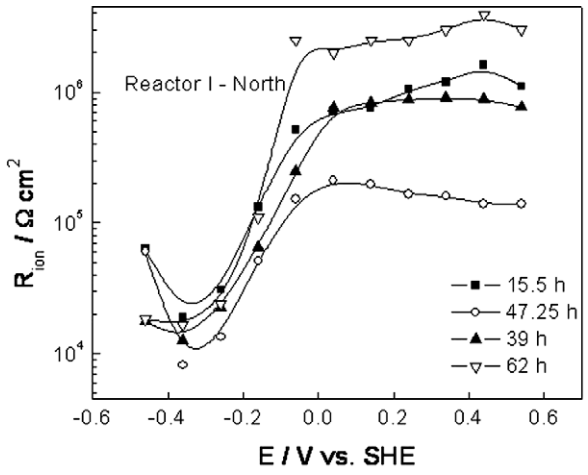

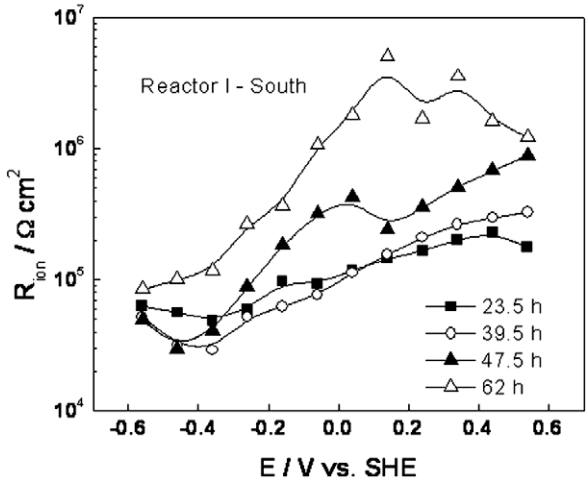

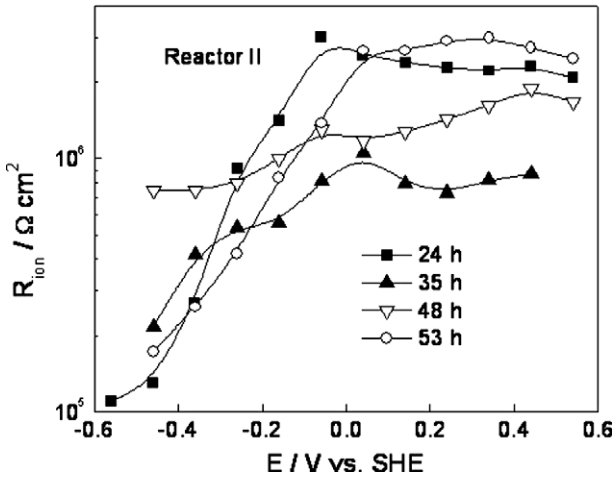

Fig. 10. Dependences of the ionic transport resistance, R_{ion}, on the applied potential for CS specimens exposed to hot conditioning environment for 15–62 h duration in different reactors.

separate study in situ impedance spectroscopy characterization was used to characterize oxidation of CS during exposure to a simulated hot conditioning water chemistry in a recirculation loop. The kinetic parameters of oxidation extracted through modelling showed that both the electric and transport properties of the oxide change with the oxidation time and stabilise after ca. 30–40

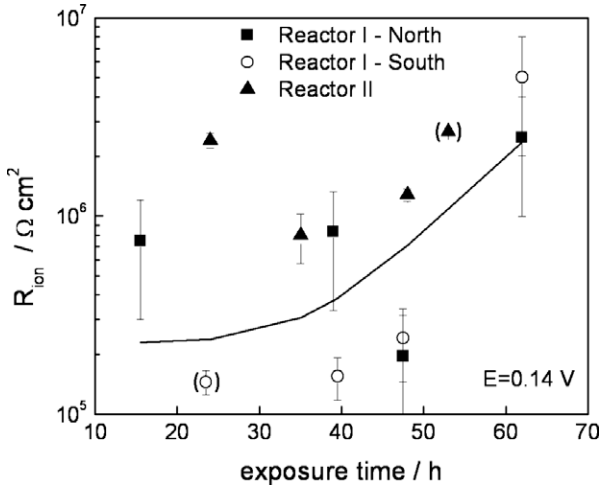

Fig. 11. Dependence of the ionic transport resistance at $E = 0.14$ V vs. SHE on the time of exposure in different reactors.

h of exposure [5]. Therefore, the results/observations of the present study and their correlation with earlier studies through a combination of different techniques clearly bring up one point – that electrochemical impedance spectroscopic measurements of oxide layers formed during hot conditioning combined with adequate modelling can be a very good supplementary tool to the weight change and morphological observations in order to estimate the optimum time required for a stable magnetite film to form on carbon steel. This in turn gives better confidence on the termination of hot conditioning process after an appropriate period.

4. Conclusion

The present study involved electrochemical impedance spectroscopic characterization and structural/morphological studies on oxide film developed on carbon steel surface during exposure to hot conditioning environment of two Indian PHWR. Following are the conclusions drawn on the basis of present observations and their correlation with studies in the literature:

1. The exposure of carbon steel coupons to hot conditioning environment (lithiated water at a pH of 10.4, <10 ppb O_2, ~250 °C and 7 MPa pressure) did result in the formation of pure magnetite phase on the surface.
2. The magnetite layer grown on CS exhibited gradual enhancement of coverage and uniformity and had a completely uniform morphology after 35 h exposure.
3. The defect density levels extracted from impedance spectroscopy measurements though high at initial exposures decreased with time and saturated/stabilised after an exposure of 35 h, whereas the values of the ionic transport resistance start to increase after 35–40 h of exposure. This observation correlated well with literature studies on stabilisation of magnetite layer arrived at using other techniques. The quantitative level of defect densities ($\sim 3 \times 10^{21}$ cm^{-3}) and ionic transport resistances also matched well with literature.
4. The observation of the current studies highlights the usefulness/applicability of electrochemical impedance spectroscopy technique as a supplementary tool to the thickness and morphological observation through microscopy to arrive at a reliable estimate of the exposure time needed for growth of a stabilised, fully covering and adherent magnetite layer on CS during hot conditioning.

References

[1] G.C. Shah, S.K. Ghosal, V. Kain, A.K. Sriraman, R.C. Khandelwal, in: Proceedings of the Symposium on Current Trends in Water Chemistry of Nuclear and Thermal Power Plants and Other Related Units (CURTWAC-95), Mumbai, February 13–16, Bhabha Atomic Research Centre, 1995, pp. 93–95.
[2] G.C. Shah, S.K. Ghosal, V. Kain, A.K. Sriraman, R.C. Khandelwal, in: Proceedings of the Symposium on Current Trends in Water Chemistry of Nuclear and Thermal Power Plants and Other Related Units (CURTWAC-95), Mumbai, February 13–16, Bhabha Atomic Research Centre, 1995, pp. 95–98.
[3] V. Kain, K.B. Gaonkar, S.K. Ghosal, H.S. Gadiyar, in: Proceedings of the Symposium on Current Trends in Water Chemistry of Nuclear and Thermal Power Plants and Other Related Units (CURTWAC-95), Mumbai, February 13–16, Bhabha Atomic Research Centre, 1995, pp. 110–111.
[4] K.B. Gaonkar, Kiran Kumar, V. Kain, H.R. Bhat, in: Proceedings of Symposium on Operational and Environmental Issues Concerning use of Water as a Coolant in Power Plants and Industries (OPENWAC-2008), Held During 15–16 December, Kalpakkam, 2008, pp. 184–188.
[5] M. Bojinov, K. Gaonkar, S. Ghosh, V. Kain, K. Kumar, T. Saario, Corros. Sci. 51 (2009) 1146–1156.
[6] J.E. Castle, H.G. Masterson, Corros. Sci. 6 (1966) 93–104.
[7] J.E. Castle, G.M.W. Mann, Corros. Sci. 6 (1966) 253–262.
[8] L. Tomlinson, Corrosion 37 (1981) 591–596.
[9] J. Robertson, Corros. Sci. 29 (1989) 1275–1291.
[10] K.E. Heusler, B. Kusian, D. McPhail, Ber. Bunsenges. Phys. Chem. 94 (1990) 1443–1449.
[11] P.S. Joshi, G. Venkateswaran, K.S. Venkateswarlu, Corrosion 48 (1992) 501–508.
[12] P.S. Joshi, G. Venkateswaran, K.S. Venkateswarlu, Corros. Sci. 34 (1993) 1367–1379.
[13] J. Trefz, M. Schweinsberg, T. Reier, J.W. Schultze, Mater. Corros. 47 (1996) 475–485.
[14] N. Arbeau, H. Allsop, R.H. Campbell, D.H. Lister, Corrosion 54 (1998) 459–468.
[15] G. Filoti, V. Kuncser, P. Palade, I.F. Micu, O. Crisan, Hyperfine Interact. 112 (1998) 35–38.
[16] M.P. Srinivasan, S. Bera, S.V. Narasimhan, J. Mater. Sci. Technol. 15 (1999) 473–477.
[17] N. Fujita, C. Matsuura, K. Saigo, Radiat. Phys. Chem. 58 (2000) 139–147.
[18] Y.-J. Kim, Corrosion 58 (2002) 108–112.
[19] B. Beverskog, M. Bojinov, A. Englund, P. Kinnunen, T. Laitinen, K. Mäkelä, T. Saario, P. Sirkiä, Corros. Sci. 44 (2002) 1901–1921.
[20] B. Beverskog, M. Bojinov, P. Kinnunen, T. Laitinen, K. Mäkelä, T. Saario, Corros. Sci. 44 (2002) 1923–1940.
[21] M. Bojinov, P. Kinnunen, T. Laitinen, K. Mäkelä, T. Saario, P. Sirkiä, Electrochem. Commun. 4 (2002) 222–226.
[22] Y.F. Cheng, J. Bullerwell, F.R. Steward, Electrochim. Acta 48 (2003) 1521–1530.
[23] Y.F. Cheng, F.R. Steward, Corros. Sci. 46 (2004) 2405–2420.
[24] C.S. Kumai, T.M. Devine, Corrosion 61 (2005) 201–218.
[25] V. Malinovschi, C. Ducu, N. Aldea, M. Fulger, J. Nucl. Mater. 352 (2006) 107–115.
[26] R.M. Cornell, U. Schwertmann, The Iron Oxides, second ed., Wiley-VCH, 2003.
[27] J.H. Kennedy, K.W. Frese Jr., J. Electrochem. Soc. 125 (1978) 723–726.
[28] C. Gleitzer, Key Eng. Mater. 125-126 (1997) 355–418.
[29] J.B. Wagner, K.R. Lawless, A.T. Gwathmey, Trans. Metall. Soc. 221 (1961) 257.
[30] U.R. Evans, The Corrosion and Oxidation of Metals Scientific Principles and Practical Applications, Arnold, London, 1971.
[31] M. Seo, J.B. Lumsden, R.W. Staehle, Surf. Sci. 50 (1975) 541–552.
[32] J. Wielant, V. Goo ssens, R. Hausbrand, H. Terryn, Electrochim. Acta 52 (2007) 7617–7625.
[33] D.D. Macdonald, J. Electrochem. Soc. 139 (12) (1992) 3434–3449.
[34] T. Zimina, E. Oshe, V. Dubkov, P. Zimin, E. Zabrodskaya, J. Electrochem. Soc. 145 (7) (1998) 2236–2240.
[35] L. Young, Trans. Faraday Soc. 51 (1955) 1250–1260.
[36] M. Bojinov, G. Fabricius, T. Laitinen, K. Mäkelä, T. Saario, G. Sundholm, Electrochim. Acta 46 (2001) 1339–1358.